DGLAP EVOLUTION OF TRUNCATED MOMENTS OF PARTON DENSITIES WITHIN TWO DIFFERENT APPROACHES

Dorota Kotlorz

Department of Physics, Technical University of Opole
Ozimska 75, 45-370 Opole, Poland
dstrozik@po.opole.pl

Andrzej Kotlorz

Department of Mathematics, Technical University of Opole
Luboszycka 3, 45-370 Opole, Poland

(Received July 1, 2005; revised version received August 8, 2005)

We solve the LO DGLAP QCD evolution equation for truncated Mellin moments of the nucleon nonsinglet structure function. The results are compared with those, obtained in the Chebyshev-polynomial approach for x-space solutions. Computations are performed for a wide range of the truncation point $10^{-5} \leq x_0 \leq 0.9$ and $1 \leq Q^2 \leq 100$ GeV^2. The agreement is perfect for higher moments ($n \geq 2$) and not too large x_0 ($x_0 \leq 0.1$), even for a small number of terms in the truncated series ($M = 4$). The accuracy of the truncated moments method increases for larger M and decreases very slowly with increasing Q^2. For $M = 30$ the relative error in a case of the first moment at $x_0 \leq 0.1$ and $Q^2 = 10$ GeV^2 does not exceed 5% independently on the shape of the input parametrisation. This is a quite satisfactory result. Using the truncated moments approach one can avoid uncertainties from the unmeasurable $x \to 0$ region and also study scaling violations without making any assumption on the shape of input parametrisation of parton distributions. Therefore the method of truncated moments seems to be a useful tool in further QCD analyses.

PACS numbers: 12.38.Bx

1. Introduction

The DGLAP evolution [1] is the most familiar resummation technique, which describes scaling violations of parton densities. Measurements of deep-inelastic scattering structure functions of the nucleon allow the determina-

tion of free parameters of the input parton distributions and the verification of so called sum rules. There exist different sum rules for unpolarised and polarised structure functions which refer to the moments of the structure functions. From a phenomenological point of view, however, QCD tests based on moments $\int_0^1 dx x^{n-1} F(x,Q^2)$ are unreliable. The limit $x \to 0$, which implies that the invariant energy W^2 of the inelastic lepton–hadron scattering becomes infinite ($W^2 = Q^2(1/x - 1)$) will never be attained experimentally. In the theoretical approach to structure functions there are two ways to avoid the problem of dealing with the unphysical region $x \to 0$. The first one is to work in x-space and obtain directly the evolution of parton distributions (not of their moments). Then one has integro-differential equations (*e.g.* DGLAP one) in x and Q^2 but the integration over x goes for $x \geq x_0$. In this case an extrapolation to the unmeasurable $x \to 0$ region is unneeded. The second way is using evolution equations for truncated moments of structure functions $\int_{x_1}^{x_2} dx x^{n-1} F(x,Q^2)$ instead of for full moments. In the usually used method of solving QCD evolution equations, one takes the Mellin (full) transform of these equations and obtains analytical solutions. Then after the inverse Mellin transform (performed numerically) one has suitable solutions of the original equations in x-space. In this way *e.g.* in a case of DGLAP approximation, the differentio-integral equations for parton distributions $q(x,Q^2)$ change after the Mellin transform into simple differential and diagonalised ones in the moment space n. The only problem is knowledge of the input parametrisation for the whole region $0 \leq x \leq 1$ what is necessary in the determination of the initial moments of the distribution functions. Using truncated moments approach one can avoid uncertainties from the unmeasurable $x \to 0$ region and also obtain important theoretical results incorporating perturbative QCD effects at small x, which could be verified experimentally. Truncated moments of parton distributions in solving DGLAP equations have been presented in [3]. Authors have shown that the evolution equations for truncated moments though not diagonal can be solved with a quite good precision for $n \geq 2$. This is because each n-th truncated moment couples only with $(n+j)$-th ($j \geq 0$) truncated moments. In [5] the truncated moments method has been adopted to double logarithmic $\ln^2 x$ resummation. There is a number of papers in which the most known methods for solving the Q^2 evolution equations for parton distributions have been reviewed (see *e.g.* [6, 7]). Authors compare the DGLAP framework for the full Mellin moments method with brute-force or Laguerre-polynomial approaches, used for x-space version of the evolution equation. In this paper we compare the solutions of LO DGLAP Q^2 evolution equations written for the truncated Mellin moments of the structure functions with those, obtained by using the Chebyshev-polynomial method in the x-space. In both these approaches we compute the truncated mo-

ments $\int_{x_0}^1 dx x^{n-1} F(x,Q^2)$. As a test structure function $F(x,Q^2)$ we take two different spin-like nonsinglet parton distributions. We perform the computations for a wide range of the truncation point $10^{-5} \leq x_0 \leq 0.9$ and $1 \leq Q^2 \leq 100$ GeV^2. In the next section we briefly recall an idea of the evolution equation for truncated moments of parton distributions. The main topic of our paper *i.e.* the comparison of the Chebyshev-polynomial and truncated moments techniques in solving the LO DGLAP evolution equation for the nonsinglet structure function is presented in Section 3. Finally, Section 4 contains conclusions.

2. Truncated Mellin moments of the nonsinglet structure function $q^{\mathbf{NS}}(x,t)$ within LO DGLAP approach

For (full) Mellin moments of parton distributions $f(x,Q^2)$

$$\bar{f}(n,Q^2) = \int_0^1 dx x^{n-1} f(x,Q^2) \tag{2.1}$$

the DGLAP evolution equation can be solved analytically. This is because one obtains in the moment space n simple diagonalised differential equations. The only problem is the knowledge of the input parametrisation for the whole region $0 \leq x \leq 1$, what is necessary in the determination of the initial moments $\bar{f}(n,Q^2 = Q_0^2)$:

$$\bar{f}(n,Q_0^2) = \int_0^1 dx x^{n-1} f(x,Q_0^2)\,. \tag{2.2}$$

Using the truncated moments approach one can avoid the uncertainties from the region $x \to 0$, which will never be attained experimentally. The derivation of the DGLAP equations for truncated moments of parton distributions has been presented in [3]. The evolution equations for truncated moments $\bar{f}(x_0,n,Q^2)$ are not diagonal and therefore solving this problem is not so easy like in a case of the full-moments technique. Nevertheless this method has an advantage over other approaches, based not only on the cut-off for unphysical region $x \to 0$. The technique of truncated moments within DGLAP approximation enables namely to study scaling violations without making any assumption on the shape of the input parametrisation of parton distributions. While the solution of the evolution equations in the x-space requires knowledge of inputs $f(x,Q_0^2)$ with many parameters (fitted in detailed comparison with the data), the initial values of truncated moments can be obtained directly by data. Following the authors of [3], we have found

the LO DGLAP evolution equation for the truncated at x_0 Mellin moment of the nonsinglet structure function $q^{\rm NS}(x,Q^2)$ in a form:

$$\frac{d\bar{q}^{\rm NS}(x_0,n,t)}{dt} = \frac{\alpha_{\rm s}(t)}{2\pi}\int\limits_{x_0}^{1} dy y^{n-1} q^{\rm NS}(y,t) G_n\left(\frac{x_0}{y}\right). \tag{2.3}$$

$\bar{q}^{\rm NS}(x_0,n,t)$ is the truncated at x_0 moment of the nonsinglet structure function:

$$\bar{q}^{\rm NS}(x_0,n,t) = \int\limits_{x_0}^{1} dx x^{n-1} q^{\rm NS}(x,t)\,, \tag{2.4}$$

where

$$t \equiv \ln\frac{Q^2}{\Lambda^2_{\rm QCD}} \tag{2.5}$$

and

$$G_n\left(\frac{x_0}{y}\right) \equiv \int\limits_{x_0/y}^{1} dz z^{n-1} P_{qq}(z)\,. \tag{2.6}$$

For $x_0 = 0$ the kernel $G_n(x_0/y)$ is simply equal to the anomalous dimension $\gamma_{qq}(n)$:

$$\gamma_{qq}(n) = \int\limits_{0}^{1} z^{n-1} P_{qq}(z) dz\,. \tag{2.7}$$

Expanding the G_n in Taylor series around $y = 1$, one has

$$\begin{aligned} G_n\left(\frac{x_0}{y}\right) \;=\; & \gamma_{qq}(n) - \frac{4}{3}\sum_{k=0}^{\infty}\left[2\sum_{i=n+2}^{\infty}\frac{(i+k-1)!}{i!}x_0^i \right. \\ & \left. + \frac{(n+k-1)!}{n!}\left(x_0^n + \frac{n+k}{n+1}x_0^{n+1}\right)\right]\sum_{p=0}^{k}\frac{(-1)^p y^p}{p!(k-p)!}\,. \end{aligned} \tag{2.8}$$

Truncating the above expansion at order M and using the following relation

$$\sum_{k=0}^{M}\sum_{p=0}^{k} \longrightarrow \sum_{p=0}^{M}\sum_{k=p}^{M} \tag{2.9}$$

one can find that the evolution equation (2.3) becomes

$$\frac{d\bar{q}^{\rm NS}(x_0,n,t)}{dt} = \frac{\alpha_{\rm s}(t)}{2\pi}\sum_{p=0}^{M} C_{pn}^{(M)}(x_0)\,\bar{q}^{\rm NS}(x_0,n+p,t) \tag{2.10}$$

and

$$G_n\left(\frac{x_0}{y}\right) = \sum_{p=0}^{M} C_{pn}^{(M)}(x_0)\, y^p\,, \tag{2.11}$$

where

$$\begin{aligned} C_{pn}^{(M)}(x_0) \;=\; & \gamma_{qq}(n)\delta_{p0} - \frac{4}{3}\sum_{k=p}^{M}\frac{(-1)^p}{p!(k-p)!}\Bigg[2\sum_{i=n+2}^{\infty}\frac{(i+k-1)!}{i!}x_0^i \\ & + \frac{(n+k-1)!}{n!}\left(x_0^n + \frac{n+k}{n+1}x_0^{n+1}\right)\Bigg]. \end{aligned} \tag{2.12}$$

Note that the evolution equations for truncated moments (2.10), (2.12) are not diagonal but each n-th moment couples only with $(n+p)$-th ($p \geq 0$) moments. As it was shown in [3] the series of couplings to higher moments is convergent and furthermore the value of $(n+p)$-th moments decreases rapidly in comparison to the n-th moment. Hence one can retain from (2.10) the closed system of $M+1$ equations:

$$\begin{aligned} &\frac{d\bar{q}^{\rm NS}(x_0,N_0,t)}{dt} = \frac{\alpha_{\rm s}(t)}{2\pi}\Big[C_{0,N_0}^{(M)}(x_0)\bar{q}^{\rm NS}(x_0,N_0,t) \\ &+C_{1,N_0}^{(M)}(x_0)\bar{q}^{\rm NS}(x_0,N_0+1,t)+\ldots+C_{M,N_0}^{(M)}(x_0)\bar{q}^{\rm NS}(x_0,N_0+M,t)\Big], \\ &\frac{d\bar{q}^{\rm NS}(x_0,N_0+1,t)}{dt} = \frac{\alpha_{\rm s}(t)}{2\pi}\Big[C_{0,N_0+1}^{(M-1)}(x_0)\bar{q}^{\rm NS}(x_0,N_0+1,t) \\ &+C_{1,N_0+1}^{(M-1)}(x_0)\bar{q}^{\rm NS}(x_0,N_0+2,t)+\ldots+C_{M-1,N_0+1}^{(M-1)}(x_0)\bar{q}^{\rm NS}(x_0,N_0+M,t)\Big], \\ &\qquad\qquad\qquad\qquad\qquad\qquad\ldots \\ &\frac{d\bar{q}^{\rm NS}(x_0,N_0+M,t)}{dt} = \frac{\alpha_{\rm s}(t)}{2\pi}C_{0,N_0+M}^{(0)}(x_0)\bar{q}^{\rm NS}(x_0,N_0+M,t)\,. \end{aligned} \tag{2.13}$$

N_0 denotes the lowest moment in calculations. The above system can be solved numerically like a standard coupled differential equations using the Runge–Kutta method. We have also found an analytical solution of (2.13) in the form:

$$\begin{aligned} \bar{q}^{\rm NS}(x_0,i,t) = & \left(\bar{q}^{\rm NS}(x_0,i,t_0) - \sum_{k=i+1}^{N_0+M}A_{ik}(x_0)\bar{q}^{\rm NS}(x_0,k,t_0)\right) \\ & \times\exp\left(\frac{\alpha_{\rm s}}{2\pi}D_{ii}^{(M)}(x_0)(t-t_0)\right) + \sum_{k=i+1}^{N_0+M}A_{ik}(x_0)\bar{q}^{\rm NS}(x_0,k,t) \end{aligned} \tag{2.14}$$

for $\alpha_{\rm s} = {\rm const}$ and

$$\bar{q}^{\rm NS}(x_0,i,t) = \left(\bar{q}^{\rm NS}(x_0,i,t_0) - \sum_{k=i+1}^{N_0+M} A_{ik}(x_0)\bar{q}^{\rm NS}(x_0,k,t_0)\right) \times \exp\left(c_f D_{ii}^{(M)}(x_0)\ln\frac{t}{t_0}\right) + \sum_{k=i+1}^{N_0+M} A_{ik}(x_0)\bar{q}^{\rm NS}(x_0,k,t) \qquad (2.15)$$

for the running $\alpha_{\rm s}$. Matrix elements $D_{ij}^{(M)}(x_0)$ and $A_{ij}(x_0)$ are given in Appendix B. For details about properties of triangular matrices like D see also [3]. We have made sure that the results (2.14), (2.15) agree with the solutions obtained with the help of the Runge–Kutta method. In the forthcoming chapter we compare predictions for the truncated moments $\bar{q}^{\rm NS}(x_0,n,t)$ obtained by solving Eq. (2.13) with those, computed in the Chebyshev polynomial approach.

3. Results for truncated moments of the nonsinglet structure function $\bar{q}^{\rm NS}(x_0,n,t)$ within LO approximation of the DGLAP approach

We solve the system of evolution equations for truncated moments (2.13) and compare the results with predictions, obtained in the Chebyshev polynomial approach. The Chebyshev polynomials technique [10] was successfully used by J. Kwieciński in many QCD treatments *e.g.* [2,8]. Using this method one obtains the system of linear differential equations instead of the original integro-differential ones. The Chebyshev expansion provides a robust method of discretising a continuous problem. This allows computing the parton distributions for "not too singular" input parametrisation in the whole $x \in (0;1)$ region. More detailed description of the Chebyshev polynomials method in the solving the QCD evolution equations is given in Appendix A. In this paper we use two spin-like input parametrisations of the parton distribution $q^{\rm NS}(x,Q_0^2)$ at $Q_0^2 = 1\ {\rm GeV}^2$, namely:

$$q^{\rm NS}(x,Q_0^2) \;=\; a_1(1-x)^3, \qquad (3.1)$$

$$q^{\rm NS}(x,Q_0^2) \;=\; a_2 x^{-0.4}(1-x)^{2.5}\,, \qquad (3.2)$$

where constants a_1 and a_2 are determined by the appropriate sum rules. More singular at small-x input (3.2) incorporates the latest knowledge about the low-x behaviour of the polarised structure functions [9]. We start our analysis with a simple test, where the truncation point $x_0 = 0$. Then the results should be, of course, equal to the analytical ones:

$$\bar{q}^{\rm NS}(n,Q^2) = \bar{q}^{\rm NS}(n,Q_0^2)\left(\frac{\alpha_{\rm s}(Q_0^2)}{\alpha_{\rm s}(Q^2)}\right)^{c_f\gamma_{qq}(n)}. \qquad (3.3)$$

$\alpha_s(Q^2)$ is the running coupling and c_f depends on the number of the quark flavours N_f:

$$c_f = \frac{2}{11 - \frac{2}{3}N_f}\,. \tag{3.4}$$

Table I shows the analytical values of full moments $\bar{q}^{\rm NS}(n,t)$ for two values

TABLE I

Test of the Chebyshev polynomial method: comparison with analytical results of n-th (full) moments $\bar{q}^{\rm NS}(n,Q^2)$ for different Q^2 and input functions $q^{\rm NS}(x,Q_0^2)$.

$q^{\rm NS}(x,Q_0^2)$	Q^2	n	$\bar{q}^{\rm NS}(n,Q^2)$	$\Delta_{\rm Cheb}\%$
$a_1(1-x)^3$	100	1	2.112×10^{-1}	$<4\times10^{-1}$
		2	2.820×10^{-2}	$<4\times10^{-2}$
		3	7.492×10^{-3}	$<2\times10^{-1}$
		4	2.732×10^{-3}	$<3\times10^{-1}$
		5	1.204×10^{-3}	$<7\times10^{-1}$
	10	1	2.112×10^{-1}	$<2\times10^{-1}$
		2	3.296×10^{-2}	$<2\times10^{-2}$
		3	9.556×10^{-3}	$<5\times10^{-2}$
		4	3.709×10^{-3}	$<2\times10^{-1}$
		5	1.716×10^{-3}	$<3\times10^{-1}$
$a_2x^{-0.4}(1-x)^{2.5}$	100	1	2.112×10^{-1}	<2
		2	2.098×10^{-2}	$<5\times10^{-2}$
		3	5.245×10^{-3}	$<2\times10^{-1}$
		4	1.902×10^{-3}	$<3\times10^{-1}$
		5	8.502×10^{-4}	<2
	10	1	2.112×10^{-1}	$<9\times10^{-1}$
		2	2.452×10^{-2}	$<2\times10^{-2}$
		3	6.691×10^{-3}	$<4\times10^{-2}$
		4	2.583×10^{-3}	$<9\times10^{-2}$
		5	1.212×10^{-3}	$<2\times10^{-1}$

of $Q^2 : 10$ GeV^2 and 100 GeV^2 together with the percentage errors for the Chebyshev results $\Delta_{\rm Cheb}\%$:

$$\Delta_{\rm Cheb}\% = \frac{\mid \bar{q}^{\rm NS}(n,t)({\rm analytical}) - \bar{q}^{\rm NS}(n,t)({\rm Chebyshev}) \mid}{\bar{q}^{\rm NS}(n,t)({\rm analytical})}\, 100\% \,. \quad (3.5)$$

Note a good agreement of the Chebyshev solutions for $\bar{q}^{\rm NS}(n,Q^2)$ in comparison to the exact analytical results. The percentage error defined in (3.5) does not exceed 1% in a case of the flat input (3.1) and 2% in a case of the more singular at small-x input (3.2). The accuracy is better for lower Q^2, when the DGLAP evolution is shorter. Using the results from Table I, we expect the similar precision for the truncated moments as well. Thus we assume that the Chebyshev method predictions are reliable with carefully estimated errors: 1% for the parametrisation (3.1) and 2% for (3.2). In Tables II and III we compare results for truncated at x_0 (0.01 and 0.1 respectively) moments, obtained from (2.15) (FMPR) with those, found within the Chebyshev approach (Cheb). We set again two scales of $Q^2 : 10$ GeV^2 and 100 GeV^2.

Notice a quite satisfactory agreement of the both presented methods even for a very small value of M (4). The accuracy of the determination of higher moments is better despite the fact, that less terms $(M-n)$ are included. The accuracy of the truncated moments method depends on the convergence of the expansion of $G_n(x_0/y)$, which is the truncated counterpart of the anomalous dimension $\gamma_{qq}(n)$. Because $G_n(x_0/y)$ is expanded in powers of y around $y=1$, the small-y region ($y \sim x_0$) in the integral of the evolution equation (2.3) is badly reproduced. Therefore, the convergence is better for higher moments, which have a smaller contribution from the low-y region. Lower moments are more sensitive to the lower limit of the integration x_0 in (2.3). From the other side, for sufficiently small x_0, factors x_0^i in the coefficients $C_{pn}^M(x_0)$ (2.12) make the convergence of $G_n(x_0/y)$ better. Hence the difference between $\bar{q}^{\rm NS}(x_0,n,Q^2)$FMPR and $\bar{q}^{\rm NS}(x_0,n,Q^2)$Cheb is larger for $x_0 = 0.1$ than for $x_0 = 0.01$. Furthermore, as $x_0 \to 1$, the accordance of $\bar{q}^{\rm NS}(x_0,n,Q^2)$FMPR and $\bar{q}^{\rm NS}(x_0,n,Q^2)$Cheb becomes again better because of the vanishing structure functions in this limit. Comparisons of $\bar{q}^{\rm NS}(x_0,n,Q^2)$FMPR with $\bar{q}^{\rm NS}(x_0,n,Q^2)$Cheb as a function of x_0 for first $(n=1)$ and second $(n=2)$ moments are shown in Figs. 1, 2. In Figs. 3–6 we present the Q^2 dependence of $\bar{q}^{\rm NS}(x_0,n,Q^2)$FMPR and $\bar{q}^{\rm NS}(x_0,n,Q^2)$Cheb at fixed $x_0 = 0.01, 0.1$ and for $n=1$, $n=2$ respectively. The plots are given for different M and both parametrisations (3.1), (3.2). The agreement of the truncated moment method with the Chebyshev approach is perfect for $n=2$ at $x_0 \le 0.01$, independently on the inputs, Q^2 and even value of M. The other results are also very satisfactory. The relative difference between $\bar{q}^{\rm NS}(x_0,n,Q^2)$FMPR and $\bar{q}^{\rm NS}(x_0,n,Q^2)$Cheb does not exceed 5% for $n \ge 2$

TABLE II

Truncated at $x_0 = 0.01$ n-th moments $\bar{q}^{\rm NS}(x_0, n, Q^2)$ within FMPR and Chebyshev approaches for different Q^2 and input functions $q^{\rm NS}(x, Q_0^2)$.

$q^{\rm NS}(x, Q_0^2)$	Q^2	n	$\bar{q}$(Cheb)	$\bar{q}$(FMPR)
$a_1(1-x)^3$	100	1	1.892×10^{-1}	2.006×10^{-1}
		2	2.812×10^{-2}	2.817×10^{-2}
		3	7.499×10^{-3}	7.491×10^{-3}
		4	2.740×10^{-3}	2.732×10^{-3}
		5	1.212×10^{-3}	1.204×10^{-3}
	10	1	1.951×10^{-1}	2.015×10^{-1}
		2	3.289×10^{-2}	3.293×10^{-2}
		3	9.561×10^{-3}	9.556×10^{-3}
		4	3.714×10^{-3}	3.709×10^{-3}
		5	1.721×10^{-3}	1.716×10^{-3}
$a_2 x^{-0.4}(1-x)^{2.5}$	100	1	1.658×10^{-1}	1.817×10^{-1}
		2	2.082×10^{-2}	2.090×10^{-2}
		3	5.250×10^{-3}	5.245×10^{-3}
		4	1.907×10^{-3}	1.902×10^{-3}
		5	8.550×10^{-4}	8.502×10^{-4}
	10	1	1.732×10^{-1}	1.826×10^{-1}
		2	2.437×10^{-2}	2.443×10^{-2}
		3	6.692×10^{-3}	6.691×10^{-3}
		4	2.585×10^{-3}	2.583×10^{-3}
		5	1.214×10^{-3}	1.212×10^{-3}

and not too large x_0 ($x_0 \leq 0.1$), already at $M = 4$. This difference for the first moment also decreases down to a few % for $M = 30$ and $x_0 = 0.1$ (for smaller x_0 the accuracy is much better). The error function

$$R_n^M(x_0, Q^2) = \frac{\left|\bar{q}^{\rm NS}(x_0, n, Q^2){\rm FMPR} - \bar{q}^{\rm NS}(x_0, n, Q^2){\rm Cheb}\right|}{\bar{q}^{\rm NS}(x_0, n, Q^2){\rm Cheb}}\, 100\% \quad (3.6)$$

TABLE III

Truncated at $x_0 = 0.1$ n-th moments $\bar{q}^{\rm NS}(x_0, n, Q^2)$ within FMPR and Chebyshev approaches for different Q^2 and input functions $q^{\rm NS}(x, Q_0^2)$.

$q^{\rm NS}(x, Q_0^2)$	Q^2	n	$\bar{q}$(Cheb)	$\bar{q}$(FMPR)
$a_1(1-x)^3$	100	1	9.921×10^{-2}	1.236×10^{-1}
		2	2.377×10^{-2}	2.567×10^{-2}
		3	7.229×10^{-3}	7.368×10^{-3}
		4	2.721×10^{-3}	2.724×10^{-3}
		5	1.210×10^{-3}	1.203×10^{-3}
	10	1	1.138×10^{-1}	1.294×10^{-1}
		2	2.883×10^{-2}	3.011×10^{-2}
		3	9.303×10^{-3}	9.401×10^{-3}
		4	3.695×10^{-3}	3.699×10^{-3}
		5	1.719×10^{-3}	1.715×10^{-3}
$a_2 x^{-0.4}(1-x)^{2.5}$	100	1	7.112×10^{-2}	9.086×10^{-2}
		2	1.664×10^{-2}	1.816×10^{-2}
		3	5.003×10^{-3}	5.116×10^{-3}
		4	1.890×10^{-3}	1.895×10^{-3}
		5	8.536×10^{-4}	8.497×10^{-4}
	10	1	8.237×10^{-2}	9.519×10^{-2}
		2	2.026×10^{-2}	2.131×10^{-2}
		3	6.446×10^{-3}	6.528×10^{-3}
		4	2.568×10^{-3}	2.572×10^{-3}
		5	1.213×10^{-3}	1.211×10^{-3}

grows very slowly with Q^2 (see Figs. 3, 5, 6). In Tables IV and V we show the error function $R_n^M(x_0, Q^2)$ for different M, $Q^2 = 10$ GeV^2 and two values of x_0 : $0.01, 0.1$, respectively. Note that with increasing M the accuracy of the truncated moments method systematically though slowly increases. This improvement of the accuracy breaks however for larger M ($M \simeq 70$ at $x_0 = 0.01$ and $M \simeq 40$ at $x_0 = 0.1$) because of increasing numerical errors. All presented above results concern the running coupling $\alpha_{\rm s}(Q^2)$.

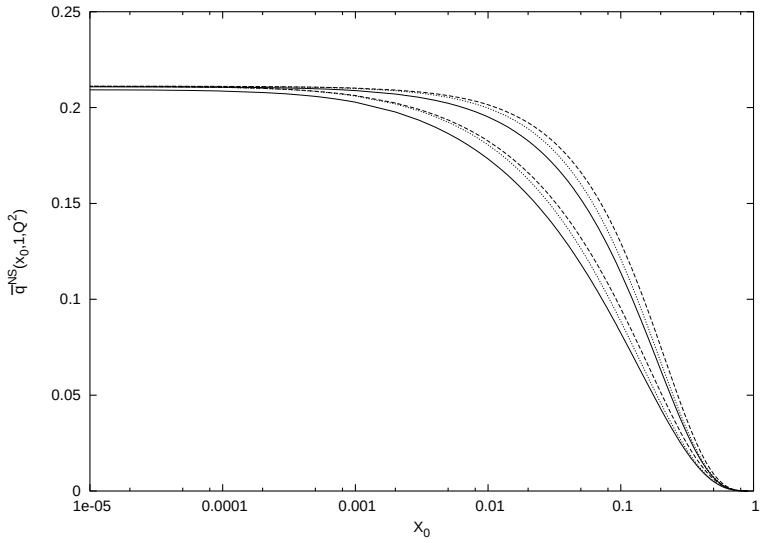

Fig. 1. First truncated moment: $\bar{q}^{\rm NS}(x_0,1,Q^2)$Cheb (solid), $\bar{q}^{\rm NS}(x_0,1,Q^2)$FMPR (dashed $M=4$, dotted $M=20$) for different inputs: (3.1) — upper lines and (3.2) — lower lines. $Q^2=10$ GeV^2.

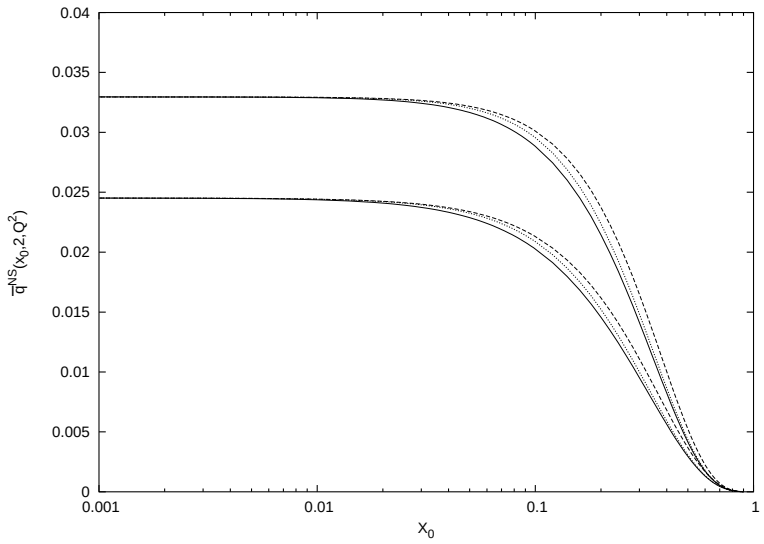

Fig. 2. Second truncated moment: $\bar{q}^{\rm NS}(x_0,2,Q^2)$Cheb (solid), $\bar{q}^{\rm NS}(x_0,2,Q^2)$FMPR (dashed $M=4$, dotted $M=20$) for different inputs: (3.1) — upper lines and (3.2) — lower lines. $Q^2=10$ GeV^2.

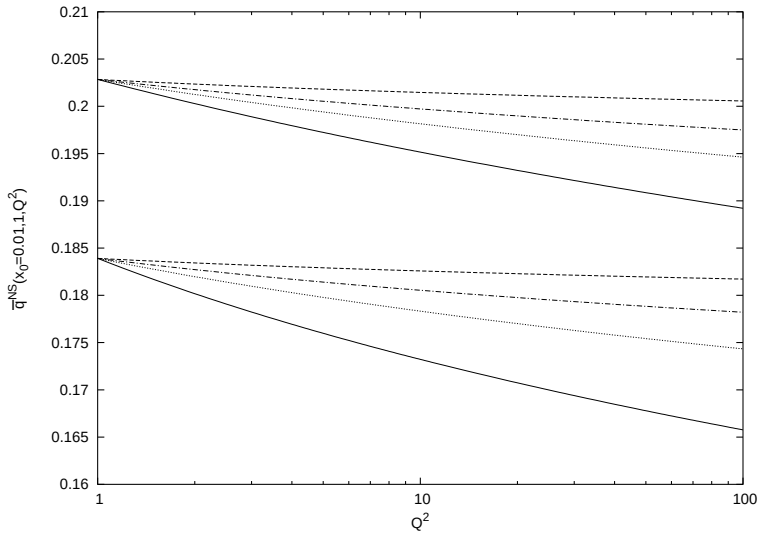

Fig. 3. First truncated at $x_0 = 0.01$ moment: $\bar{q}^{\mathrm{NS}}(x_0, 1, Q^2)$Cheb (solid), $\bar{q}^{\mathrm{NS}}(x_0, 1, Q^2)$FMPR (dashed $M = 4$, dashed-dotted $M = 20$, dotted $M = 60$). The upper lines correspond to the input parametrisation (3.1), the lower ones to (3.2).

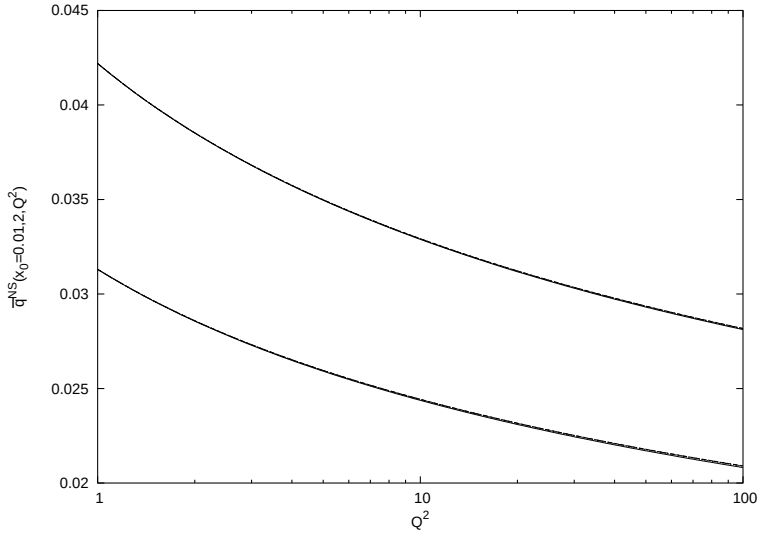

Fig. 4. Second truncated at $x_0 = 0.01$ moment: $\bar{q}^{\mathrm{NS}}(x_0, 2, Q^2)$Cheb (solid), $\bar{q}^{\mathrm{NS}}(x_0, 2, Q^2)$FMPR (covered with Cheb for different $M \geq 4$). The upper line corresponds to the input parametrisation (3.1), the lower one to (3.2).

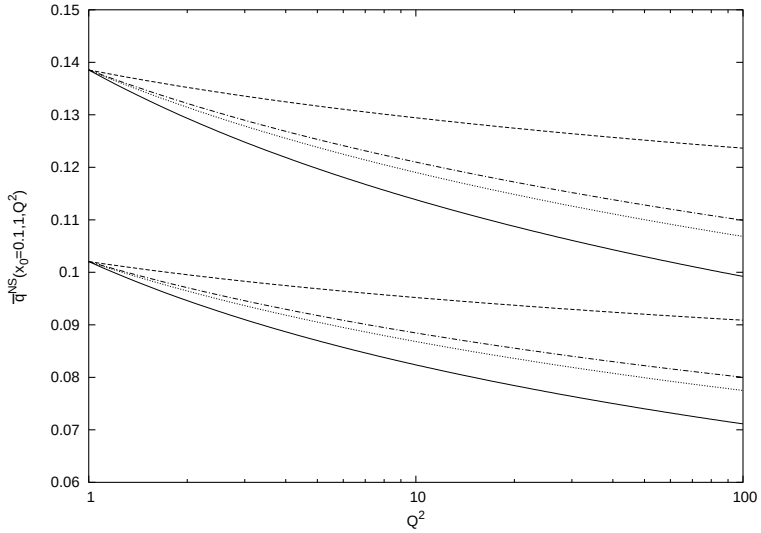

Fig. 5. First truncated at $x_0 = 0.1$ moment: $\bar{q}^{\rm NS}(x_0, 1, Q^2)$Cheb (solid), $\bar{q}^{\rm NS}(x_0, 1, Q^2)$FMPR (dashed $M = 4$, dashed–dotted $M = 20$, dotted $M = 60$). The upper lines correspond to the input parametrisation (3.1), the lower ones to (3.2).

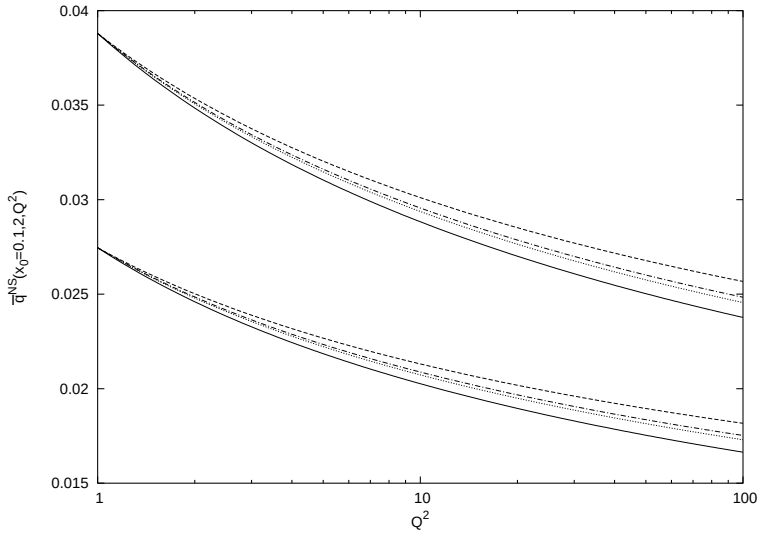

Fig. 6. Second truncated at $x_0 = 0.1$ moment: $\bar{q}^{\rm NS}(x_0, 2, Q^2)$Cheb (solid), $\bar{q}^{\rm NS}(x_0, 2, Q^2)$FMPR (dashed $M = 4$, dashed–dotted $M = 20$, dotted $M = 60$). The upper lines correspond to the input parametrisation (3.1), the lower ones to (3.2).

TABLE IV

The percentage error function $R_n \equiv R_n^M(x_0, Q^2)$ defined in (3.6), for $x_0 = 0.01$ and different input functions $q^{\mathrm{NS}}(x, Q_0^2)$. $Q^2 = 10\ \mathrm{GeV}^2$, the values of n and M shown.

$x_0 = 0.01$	$a_1(1-x)^3$		$a_2 x^{-0.4}(1-x)^{2.5}$	
M	R_1	R_2	R_1	R_2
4	4	$\ll 1$	6	$\ll 1$
10	3	$\ll 1$	5	$\ll 1$
20	3	$\ll 1$	5	$\ll 1$
30	2	$\ll 1$	4	$\ll 1$
60	2	$\ll 1$	3	$\ll 1$

TABLE V

The percentage error function $R_n \equiv R_n^M(x_0, Q^2)$ defined in (3.6), for $x_0 = 0.1$ and different input functions $q^{\mathrm{NS}}(x, Q_0^2)$. $Q^2 = 10\ \mathrm{GeV}^2$, the values of n and M shown.

$x_0 = 0.1$	$a_1(1-x)^3$		$a_2 x^{-0.4}(1-x)^{2.5}$	
M	R_1	R_2	R_1	R_2
4	13	5	16	5
10	10	4	11	4
20	6	3	7	3
30	4	2	5	2

We have found also, that for the constant α_{s} the error function R (3.6) grows approximately proportionally to the strength of α_{s}:

$$\frac{R(\alpha_{\mathrm{s}1})}{R(\alpha_{\mathrm{s}2})} \sim \frac{\alpha_{\mathrm{s}1}}{\alpha_{\mathrm{s}2}}\,. \tag{3.7}$$

Summarising, the LO DGLAP evolution of any truncated at $x_0 \leq 0.1$ moment of the parton distribution can be reproduced with the satisfactory accuracy, where the relative error $\leq 5\%$.

4. Summary and conclusions

Analysis of the QCD Q^2 evolution equations for truncated moments of parton distributions is very interesting both from the theoretical and experimental point of view. The truncated moments technique is complementary to the existing methods for solving the evolution equations, based on the

full moments or x-space approaches. Apart from this it refers directly to the physical values — moments (rather than to the parton distributions), what enables one to use a wide range of deep-inelastic scattering data in terms of smaller number of parameters. In this way, no assumptions on the shape of parton distributions are needed. Dealing with truncated at x_0 Mellin moments: $\int_{x_0}^1 dx x^{n-1} f(x,Q^2)$ one can also avoid uncertainty from the unmeasurable very small $x \to 0$ region.

In this paper we have compared the solutions of LO DGLAP Q^2 evolution equations written for the truncated Mellin moments of the structure functions with those, obtained by using the Chebyshev-polynomial technique. In both these approaches we have calculated numerically and semi-analytically the truncated moments $\int_{x_0}^1 dx x^{n-1} F(x,Q^2)$. As a test structure function $F(x,Q^2)$ we have taken two different spin-like nonsinglet parton distributions. The computations have been performed for a wide range of x_0 ($10^{-5} \leq x_0 \leq 0.9$) and Q^2 ($1 \leq Q^2 \leq 100$ GeV^2). Treating the Chebyshev results as exact, we have found that the truncated moments method is very promising, for any moment, together with the first one. The precision of the truncated moments approach is perfect for higher moments ($n \geq 2$) and not too large the truncation point x_0 ($x_0 \leq 0.1$), even for small $M = 4$. Larger values of M (*e.g.* $M = 30$) enables one to obtain a quite satisfactory accuracy (the relative error $\leq 5\%$) also for the first truncated moment. The original truncated moments technique [3] has been developed in [4], what could improve the numerical efficiency. This technique can be a valuable tool *e.g.* in determination of the contribution to the moments of the gluon distribution from the experimentally accessible region. We think that the method of truncated moments can be useful in further theoretical and experimental QCD investigations.

Appendix A

Chebyshev polynomial expansion within LO DGLAP evolution equations

In order to solve the integro-differential evolution equation

$$\frac{\partial q^{\rm NS}(x,t)}{\partial t} = \frac{\alpha_{\rm s}(t)}{2\pi} \int\limits_x^1 \frac{dz}{z} P_{qq}\left(\frac{x}{z}\right) q^{\rm NS}(z,t) \tag{A.1}$$

one has to expand functions $q^{\rm NS}(x,t)$ into the series of the Chebyshev polynomials:

$$q^{\rm NS}(x,t) \to q^{\rm NS}(x',t) = \frac{2}{N} \sum_{i=0}^{N-1} \sum_{k=0}^{N-1} \upsilon_i \, q^{\rm NS}(x_k,t) T_i(\tau_k) T_i(x') \,, \tag{A.2}$$

where

$$\upsilon_i = \begin{cases} 0.5 & \text{for} \quad i = 0 \\ 1 & \text{for} \quad i \geq 1 \end{cases}, \tag{A.3}$$

$$x' = \frac{2\ln x}{\ln x_{\min}} - 1\,. \tag{A.4}$$

$T_i(x)$ is the Chebyshev polynomial, defined as [10]:

$$T_i(x) = \cos(i \arccos(x)) \tag{A.5}$$

and τ_k are nodes (zeros) of the T_n:

$$\tau_k = \cos\frac{2k+1}{2n}\pi\,, \qquad k = 0, 1, 2, \ldots, n-1\,, \tag{A.6}$$

$$x_k = x_{\min}^{0.5(\tau_k+1)}\,. \tag{A.7}$$

$x_{\min}$ in (A.4) and (A.7) is the smallest value of Bjorken x, involved in the analysis. In our computations $x_{\min} = 10^{-6}$. Transformation (A.4) converts the physical x-region: $[x_{\min}; 1]$ into the $x' \in [-1; 1]$ one, suitable for the Chebyshev approximation. Integration over z in the evolution equation (A.1) with $q^{\mathrm{NS}}(x,t)$ expanded according to (A.2) leads to the system of linear differential equations:

$$\frac{dq^{\mathrm{NS}}(x_i,t)}{dt} = \sum_{j=0}^{N-1} H_{ij} q^{\mathrm{NS}}(x_j,t)\,. \tag{A.8}$$

This system can be solved by using the standard Runge–Kutta method with initial conditions given by the input parametrisation $q^{\mathrm{NS}}(x_j,t_0)$. N in the polynomial expansion (A.2) is equal to 20.

Appendix B

Analytical solution of the system of DGLAP evolution equations for truncated moments $\bar{q}^{\mathrm{NS}}(x_0,n,t)$

The closed system of $M+1$ DGLAP evolution equations for truncated moments $\bar{q}^{\mathrm{NS}}(x_0,n,t)$ (2.13) can be rewritten in the form:

$$\frac{d\bar{q}^{\mathrm{NS}}(x_0,N_0,t)}{dt} = \frac{\alpha_{\mathrm{s}}(t)}{2\pi}\Big[D^{(M)}_{N_0,N_0}(x_0)\bar{q}^{\mathrm{NS}}(x_0,N_0,t)$$
$$+D^{(M)}_{N_0,N_0+1}(x_0)\bar{q}^{\mathrm{NS}}(x_0,N_0+1,t) + \ldots + D^{(M)}_{N_0,N_0+M}(x_0)\bar{q}^{\mathrm{NS}}(x_0,N_0+M,t)\Big],$$

$$\frac{d\bar{q}^{\rm NS}(x_0,N_0+1,t)}{dt}=\frac{\alpha_{\rm s}(t)}{2\pi}\Big[D^{(M-1)}_{N_0+1,N_0+1}(x_0)\bar{q}^{\rm NS}(x_0,N_0+1,t)$$
$$+D^{(M-1)}_{N_0+1,N_0+2}(x_0)\bar{q}^{\rm NS}(x_0,N_0+2,t)+\ldots+D^{(M-1)}_{N_0+1,N_0+M}(x_0)\bar{q}^{\rm NS}(x_0,N_0+M,t)\Big],$$
$$\ldots$$
$$\frac{d\bar{q}^{\rm NS}(x_0,N_0+M,t)}{dt}=\frac{\alpha_{\rm s}(t)}{2\pi}D^{(0)}_{N_0+M,N_0+M}(x_0)\bar{q}^{\rm NS}(x_0,N_0+M,t). \qquad \text{(B.1)}$$

N_0 denotes the lowest moment in calculations and the matrix elements $D^{(k)}_{ij}(x_0)$ are related to the $C^{(k)}_{ij}(x_0)$ (2.12) via

$$D^{(k)}_{ij}(x_0)=\begin{cases} C^{(k)}_{j-i,i}(x_0) & j\geq i \\ 0 & j<i \end{cases}. \qquad \text{(B.2)}$$

D is a triangular matrix and therefore (B.1) can be solved analytically using the diagonalising matrix A:

$$A_{ij}(x_0)=\frac{D_{ij}(x_0)-\sum\limits_{k=i+1}^{j-1}D_{kj}(x_0)A_{ik}}{D_{jj}(x_0)-D_{ii}(x_0)}. \qquad \text{(B.3)}$$

In this way one obtains the recurrence solutions (2.14), (2.15).

REFERENCES

[1] V.N. Gribov, L.N. Lipatov, *Sov. J. Nucl. Phys.* **15**, 438 and 675 (1972); Yu.L. Dokshitzer, *Sov. Phys. JETP* **46**, 641 (1977); G. Altarelli, G. Parisi, *Nucl. Phys.* **B126**, 298 (1977).

[2] J. Kwieciński, M. Maul, *Phys. Rev.* **D67**, 034014 (2003).

[3] S. Forte, L. Magnea, *Phys. Lett.* **B448**, 295 (1999); S. Forte, L. Magnea, A. Piccione, G. Ridolfi, *Nucl. Phys.* **B594**, 46 (2001).

[4] A. Piccione, *Phys. Lett.* **B518**, 207 (2001).

[5] D. Kotlorz, A. Kotlorz, *Acta Phys. Pol. B* **35**, 705 (2004).

[6] P. Santorelli, E. Scrimieri, *JHEP Conf. Proc. corfu* 98/023 [hep-ph/9909289].

[7] S. Kumano, T.-H. Nagai, *J. Comput. Phys.* **201**, 651 (2004) [hep-ph/0405160].

[8] J. Kwieciński, D. Strózik-Kotlorz, *Z. Phys.* **C48**, 315 (1990); J. Kwieciński, B. Ziaja, *Phys. Rev.* **D60**, 054004 (1999); B. Badełek, J. Kwieciński, *Phys. Lett.* **B418**, 229 (1998).

[9] B.I. Ermolaev, M. Greco, S.I. Troyan, *Nucl. Phys.* **B571**, 137 (2000); hep-ph/0106317; *Nucl. Phys.* **B594**, 71 (2001); *Phys. Lett.* **B522**, 57 (2001); *Phys. Lett.* **B579**, 321 (2004); hep-ph/0404267.

[10] S.E. El-gendi, *Comput. J.* **12**, 282 (1969).